ADVANCED FUNCTIONAL MATERIALS
www.afm-journal.de

All-Natural, Degradable, Rolled-Up Straws Based on Cellulose Micro- and Nano-Hybrid Fibers

Xizheng Wang, Zhenqian Pang, Chaoji Chen, Qinqin Xia, Yubing Zhou, Shuangshuang Jing, Ruiliu Wang, Upamanyu Ray, Wentao Gan, Claire Li, Gegu Chen, Bob Foster, Teng Li, and Liangbing Hu**

Among all the plastic pollution, straws have brought particularly intricate problems since they are single use, consumed in a large volume, cannot be recycled in most places, and can never be fully degraded. To solve this problem, replacements for plastic straws are being developed following with the global trend of plastic straw bans. Nevertheless, none of the available degradable alternatives are satisfactory due to drawbacks including poor natural degradability, high cost, low mechanical performance, and poor water stability. Here, all-natural degradable straws are designed by hybridizing cellulose nanofibers and microfibers in a binder-free manner. Straws are fabricated by rolling up the wet hybrid film and sealed by the internal hydrogen bonding formed among the cellulose fibers after drying. The cellulose hybrid straws show exceptional behaviors including 1) excellent mechanical performance (high tensile strength of ≈70 MPa and high ductility with a fracture strain of 12.7%), 2) sufficient hydrostability (10× wet mechanical strength compared to commercial paper straw), 3) low cost, and 4) high natural degradability. Given the low-cost raw materials, the binder-free hybrid design based on cellulose structure can potentially be a suitable solution to solve the environmental challenges brought by the enormous usage of plastics straws.

1. Introduction

Over the past 50 years, the usage of plastics has increased rapidly, with nearly 400 million tons produced globally every year (**Figure 1**a). The widespread use of plastics, ranging from low-end food packing to high-end space exploration, is largely driven by the attractive properties of plastics, including low cost, high versatility, strength and transparency, low toxicity, and high durability.[1–3] However, the high durability has also made the abundant plastics being one of the world's grand environmental problems.[4] Nearly all commonly used plastics are not degradable or chemically reactive in the natural environment, while only 9% of the waste plastics had been recycled.[5] In practice, instead of being fully degraded, plastics break down into tiny particles that accumulate in the natural environment as wastes that have been found from the poles to the equator, and from the depths of the oceans to the tops of mountains, causing contamination of oceans, freshwater systems, and terrestrial habitats worldwide.[6–9] Common methods (i.e., reducing, reusing, and recycling) to solve the plastic waste problem have been largely ineffective. Destructive thermal treatments (e.g., combustion or pyrolysis) to eliminate plastic waste permanently are cost prohibitive and bring hazardous gas emissions and ashes.

Among all the pollutions, plastic straws have brought particularly knotty problems for the following reasons. First, the consumption of plastic straw is in a high volume (e.g., the daily consumption in US is over half billion); second, majorities of plastic straws are for single use and almost all used straws go directly into waste and then are dumped to landfill, and thus never recycled; third, even if used plastic straws go through mechanical recycling, their small size and lightweight make them hardly recyclable. As a result, the plastic straw pollution, with ≈8.3 billion ones polluting the beaches and oceans around the world, is causing rising concern globally (Figure 1b).[5,10,11] To solve this problem, there are increasing bans to plastic straws being enacted by both local governments (e.g., Washington D.C.) and large corporates (e.g., Starbucks, with ≈1 billion plastic straw consumption annually).[11] Tremendous efforts have been made in the past few decades to develop synthetic degradable and more environmental-friendly polymers. However, the progress has been far from satisfactory. Compostable polylactic acid (PLA) is the most successful given its high mechanical strength and low toxicity. However, PLA is produced from corn starch, which makes it expensive to replace

Dr. X. Wang, Dr. C. Chen, Q. Xia, Dr. Y. Zhou, S. Jing, R. Wang, Dr. W. Gan, C. Li, G. Chen, Prof. L. Hu
Department of Materials Science and Engineering
University of Maryland
College Park, MD 20742, USA
E-mail: binghu@umd.edu
Dr. X. Wang, Dr. Z. Pang, Y. Zhou, U. Ray, Prof. T. Li
Department of Mechanical Engineering
University of Maryland
College Park, MD 20742, USA
E-mail: lit@umd.edu
B. Foster
Trinity Industries, Inc.
Dallas, TX 75207, USA
The ORCID identification number(s) for the author(s) of this article can be found under https://doi.org/10.1002/adfm.201910417.

DOI: 10.1002/adfm.201910417

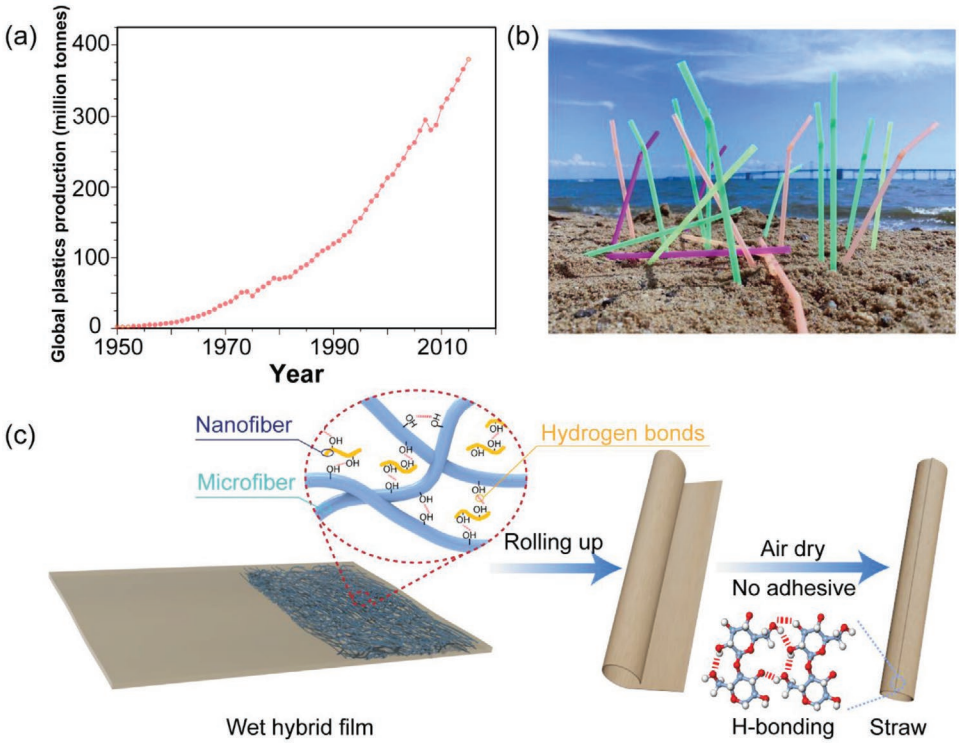

Figure 1. a) Global plastic production changing with year from 1950 to 2015. b) Photograph of plastic straws on the beach of Chesapeake Bay. c) Schematics of rolling up straw from wet cellulose hybrid film. The sealing of the straw is achieved by the formation of strong hydrogen bonding among cellulose fibers without any additional adhesive.

the low-cost petroleum-derived plastics. In addition, the degradability of PLA straws is far from acceptable since it requires specific and restrictive composting conditions for reasonable degradation time. Many efforts have been paid to develop high performance polymeric materials with exceptional mechanical properties achieved by the formation of noncovalent interlinking hydrogen bonding based on natural polymers such as silk, chitosan, and cellulose.[12,13]

Among the popular natural polymeric materials, cellulose is the most abundant on earth that can be easily degraded[14–18] and obtained at low cost. For example, bagasse, a major biowaste after sucrose extraction from sugarcane, contains 50% cellulose by mass.[14,19,20] Natural wood also contains ≈40–45% cellulose.[21–23] Cellulose fibers have diverse morphologies. Microcellulose fibers from wood and plants have an average diameter of ≈10–50 µm and a length of 1–3 mm, with a hierarchical structure comprised of nanofibrillated cellulose of an average diameter of ≈1.5–5 nm and the length can be in micrometer scale.[23–26] Due to the hierarchical structure, it is possible to produce cellulose fibers with diameters ranging from microscale to nanoscale by well-established chemical and mechanical treatments. It is noted that cellulose has remarkable intrinsic mechanical properties with a tensile strength of 2–3 GPa.[27] The density of cellulose is ≈1.5 g cm^{-3}, comparable to commonly used petroleum-derived plastics.[28] The earth abundance, low cost, lightweight, high strength, and renewable nature of cellulose make it an ideal candidate material to replace plastics. The usage of paper straws made by cellulose microfibers has seen unprecedented growth. Although can be naturally degraded, paper straws suffer many disadvantages including extremely poor water stability, high cost (due to hydrophobic wax coating), and low mechanical performance. Above said, there exist urgent needs to develop a satisfactory solution with high degradability as well as sufficient mechanical performance and water stability to replace plastic straws.

In this paper, we design degradable, all-natural cellulose-based straws composed of micro- and nano-hybrid fibers in a binder-free manner (Figure 1c). Cellulose microfibers are obtained by digesting dried bagasse in NaOH solution to remove the remaining lignin and hemicellulose. Cellulose nanofibers are prepared using a top-down chemical–mechanical approach from cellulose microfiber. Both cellulose microfibers and nanofibers can be scaled for mass production. To make straws, cellulose microfiber aqueous slurries and cellulose nanofiber suspensions are mixed well to make a wet film composed of cellulose micro- and nano- hybrid fibers with a thickness of ≈300 µm. A straw is obtained by rolling up the wet film on a polyethylene terephthalate (PET) stick which is then air dried and isolated, as shown in Figure 1c. After drying, the wall thickness of the cellulose hybrid straw shrinks to ≈150 µm. Due to the rich hydroxyl groups along the cellulose molecular chains, hydrogen bonds can be readily formed among cellulose microfibers and nanofibers. The edges of the cellulose film are adhered without adding additional additives but effectively by the newly formed hydrogen bonds among the cellulose fibers after drying. For comparison, we also fabricate two other types of straws made of pure cellulose microfibers and pure cellulose nanofibers, respectively, using the similar rolling up approach

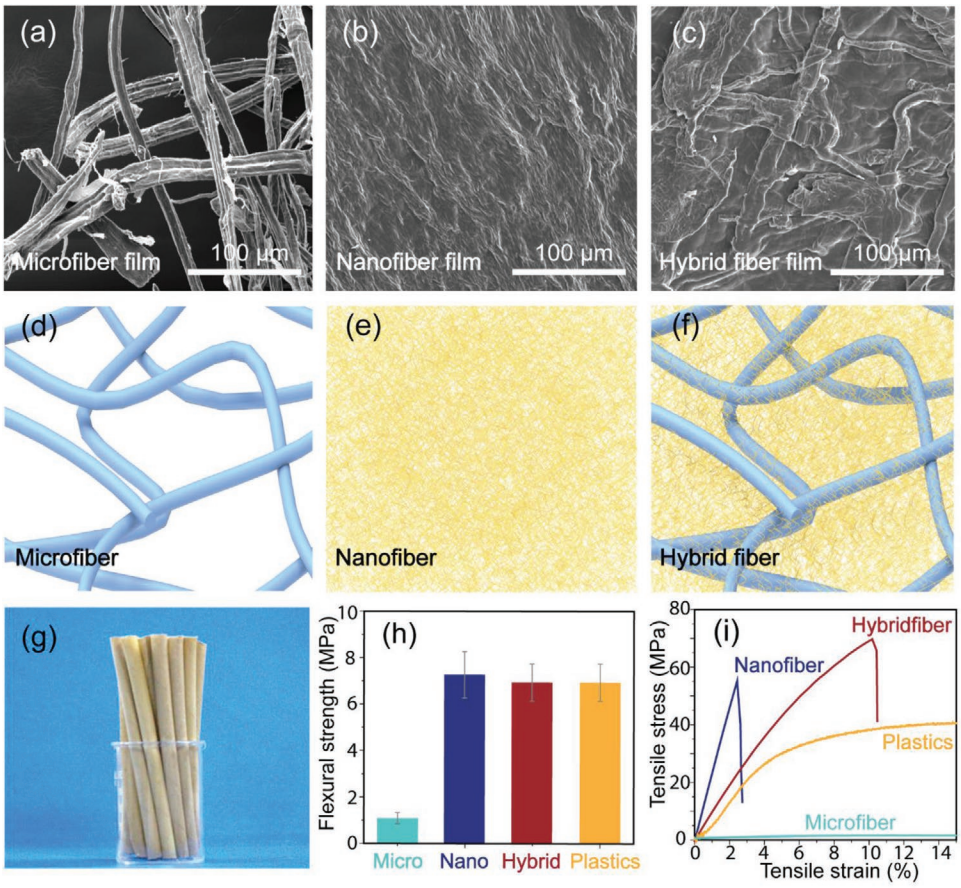

Figure 2. SEM of a) microfiber film, b) nanofiber film, and c) hybrid fiber film. Schematic morphology of d) microfiber, e) nanofiber, and f) hybrid fiber. g) A bunch of cellulose hybrid straws. h) Flexural strength comparison for microfiber straw, nanofiber straw, cellulose hybrid straw, and plastic straw. i) Tensile stress-strain curves of microfiber film, nanofiber film, cellulose hybrid film, and commercial plastic film.

(Figure S1, Supporting Information). The exceptional properties of the cellulose hybrid straws, including the 1) excellent mechanical performance (both high mechanical strength and deformability), 2) sufficient hydrostability, 3) low cost, and 4) natural degradability, bring great potential to solve the environmental problems of the plastic straws.

2. Results and Discussion

Pure cellulose microfiber straws are opaque and as soft as regular paper. Pure cellulose nanofiber straws show some optical transparence due to the densely packed nanofibers and small interstice size. The cellulose hybrid straws are opaque and have a higher mechanical strength than microfiber straws. The appearance and mechanical properties of the cellulose straws are closely related with the microscopic morphologies of the cellulose fibers. **Figure 2**a–c shows the scanning electron microscope (SEM) images of cellulose microfiber film, nanofiber film, and hybrid fiber film, respectively. As further illustrated in the schematics shown in Figure 2d–f, cellulose microfibers appear to be long (several millimeters) and thick (tens of micrometers in diameter, Figure 2a and Figure S2a (Supporting Information)) and are loosely packed with a density of only ≈0.31 g cm^{-3} (Figure S3, Supporting Information), while nanofibers are much shorter and thinner, and homogeneously and densely packed (Figure 2b) with a density increased to ≈0.94 g cm^{-3}, which is 3 times higher than that of microfiber film (Figure S3, Supporting Information). The detailed structure of cellulose nanofibers can be better revealed in the fractured surface of a nanofiber film (Figure S2b,c, Supporting Information) and in the diluted nanofiber water suspension measured by atomic force microscope (AFM) shown in Figure S4 (Supporting Information). The average diameter of nanofibers is ≈2 nm with an average length of 100–700 nm. The as-prepared nanofibers contain plenty of carboxyl groups (zeta potential = −53.2 mv, pH = 7, 0.5 wt%; Figure S5 (Supporting Information)). It was reported that at similar condition, the carboxyl group content of (2,2,6,6-tetramethylpiperidine-1-oxyl radical) TEMPO nanofibers is 1.8 mmol g^{-1}.[29] For the cellulose hybrid fiber film (Figure 2c and Figure S6 (Supporting Information)), microfibers and nanofibers are homogeneously mixed, and the nanofibers fill the voids among neighboring microfibers, resulting in a densely packed hybrid film. The density of hybrid fibers (≈0.66 g cm^{-3}) is in between of nanofibers and microfibers, which is ≈30% reduced compared with the commercial plastics (e.g., 0.99 g cm^{-3} for polypropylene, Figure S3 (Supporting Information)), bringing potential benefit for bulk

commercial product transportation. A closer look at the edge fracture on the surface of hybrid fiber film can be found in Figure S2d (Supporting Information). A bunch of cellulose hybrid straws fabricated in lab scale is shown in Figure 2g.

To investigate the mechanical performance of fabricated straws, we perform three-point bending tests of all three types of cellulose straws and compare with commercial plastic straws. Figure 2h compares the flexural strengths of three types of cellulose straws and commercial plastic straws. The cellulose microfiber straw has a low flexural strength (1.1 ± 0.2 MPa). However, both cellulose nanofiber straw and cellulose hybrid straw have a much higher flexural strength (7.3 ± 1.0 and 6.9 ± 0.8 MPa, respectively), which is comparable to or modestly higher than that of commercial plastic straws (6.9 ± 0.8 MPa). Bending flexibility is another important performance index of straws. We find that although cellulose nanofiber straws are strong, they can easily crack after bending, indicating low flexibility. Commercial plastic straws are bendable, but permanent folding marks can easily form, indicating damage of plastic material (Figure S7, Supporting Information). By contrast, both cellulose microfiber straws and cellulose hybrid straws can sustain severe bending deformation without appreciable cracking or folder marks, suggesting high bending flexibility (Figure S7, Supporting Information). The above comparison clearly shows that cellulose hybrid straws outperform cellulose nanofiber and microfiber straws, as well as commercial plastic straws, in terms of mechanical performance. The superb mechanical performance of cellulose hybrid straws against both cellulose nanofiber and microfiber straws is counterintuitive, given that the cellulose hybrid straws contain 50 wt% of microfibers.

To better understand the underlying mechanism, we perform tensile tests of the thin films of the three types of cellulose fiber structure and the thin plastic film used to make commercial plastic straw, with their stress–strain curves plotted in Figure 2i. Cellulose nanofiber film is stiff (with a stiffness of 2.3 GPa) but brittle (with a facture strain of 2.4%). Cellulose microfiber film is compliant (with a stiffness of 90 MPa) but rather ductile (with a fracture strain of 12.7%). By contrast, cellulose hybrid fiber film is sufficiently stiff (with a stiffness of ≈1 GPa) and can sustain a tensile strain up to 10.2%, leading to a desirable combination of both mechanical strength and deformability. The area underneath the stress–strain curve measures the energy needed to fracture a material (i.e., fracture energy). It is evident from Figure 2i that the cellulose hybrid fiber film has a much higher fracture energy of 4131.0 kJ m^{-3} (thus much tougher) than the cellulose nanofiber film (679.7 kJ m^{-3}) and the cellulose microfiber film (93.8 kJ m^{-3}). Figure 2i also shows that cellulose hybrid fiber film has a higher tensile strength than thin plastic film, but the thin plastic film can sustain a higher tensile strain. But, as shown in the bending test, the deformability of cellulose hybrid fiber film is sufficient to enable satisfactory bending flexibility of the resulting straw.

To shed light on mechanistic understanding of the different mechanical properties of the three types of cellulose fiber film, we carry out coarse-grained (CG) modeling to reveal the interactions between different types of cellulose fibers. The parameters of CG modeling (detailed in the Supporting Information) are obtained from the crystalline cellulose, using the full-atomistic molecular dynamics (MD) simulations. The tensile failure of cellulose fiber film is governed by the relative sliding among the cellulose fibers.[30] To capture the representative fiber-scale failure mechanism, we model the relative sliding of a cellulose fiber against six neighboring cellulose fibers patterned in a hexagonal configuration (Figure S8, Supporting Information). For the case of cellulose microfibers (or nanofibers), all the seven fibers in the CG model are cellulose microfibers (or nanofibers). For the case of cellulose hybrid fibers, certain number of neighboring microfibers are replaced by cellulose nanofibers (and thus corresponds to different micro-/nanofiber mixing ratios).

Figure 3a–c and Figures S9 and S10 (Supporting Information) plot the force per area as the function of sliding displacement, for the case of cellulose microfibers, nanofibers, and hybrid fibers with various mixing ratios. The peak value of the curve represents the material strength. The zigzag profile of all these curves corresponds to the cascade events of hydrogen bond formation, breaking, and reforming in between neighboring cellulose fibers during relative sliding.[30] The decreasing peak values of force per area in these curves result from the gradually decreasing overlapping length between the center cellulose fiber and the surrounding cellulose fibers. The maximum peak values of the force per area (often occurs in the first several peaks) give a reasonable indication of material strength (Figure S10, Supporting Information). The comparison of the curves in Figure 3 and Figure S10 (Supporting Information) shows that cellulose nanofibers have the highest strength, cellulose microfibers have the lowest strength. For the case of cellulose hybrid fibers, their strength is much higher than that of cellulose microfibers, and further increases as the nanofiber content increases. These trends agree with the experimental measurements shown in Figure 2h,i. The energy dissipated during the relative sliding of cellulose fibers measures the fracture energy.

Figure 3d compares the fracture energies of cellulose microfibers, nanofibers, and hybrid fibers with three different mixing ratios. It shows that the fracture energy of cellulose nanofibers is 17 times higher than that of cellulose microfibers, which results from the much higher stress levels during the sliding process of cellulose nanofibers. It also shows that the fracture energy of cellulose hybrid fibers could be even higher than that of cellulose nanofibers. This can be understood by the fact of the comparable stress level and significantly longer sliding distance in the case of cellulose hybrid fibers. By contrast, cellulose nanofibers can easily slide off each other due to their short length. The above CG modeling results offer mechanistic understanding of the superb mechanical performance of cellulose hybrid straws over other two types of cellulose straws.

Besides mechanical properties, hydrostability is another key performance index of straws. To compare the hydrostability of the three types of cellulose-based straws, we immerse a cellulose microfiber straw (**Figure 4**a), a cellulose nanofiber straw (Figure 4d), and a cellulose hybrid straw (Figure 4g) into water (dyed with methylene blue (10 mg mL^{-1}) for visual clarity). The cellulose microfiber straw is soaked with water and becomes soft (Figure 4b) within 30 s after being partially immersed in water, largely due to the strong capillary effect resulting from the high porosity of the cellulose microfiber film in low density (Figure 2a). However, no delamination was seen for the microfiber straw immersed in water even in 2 days, indicating

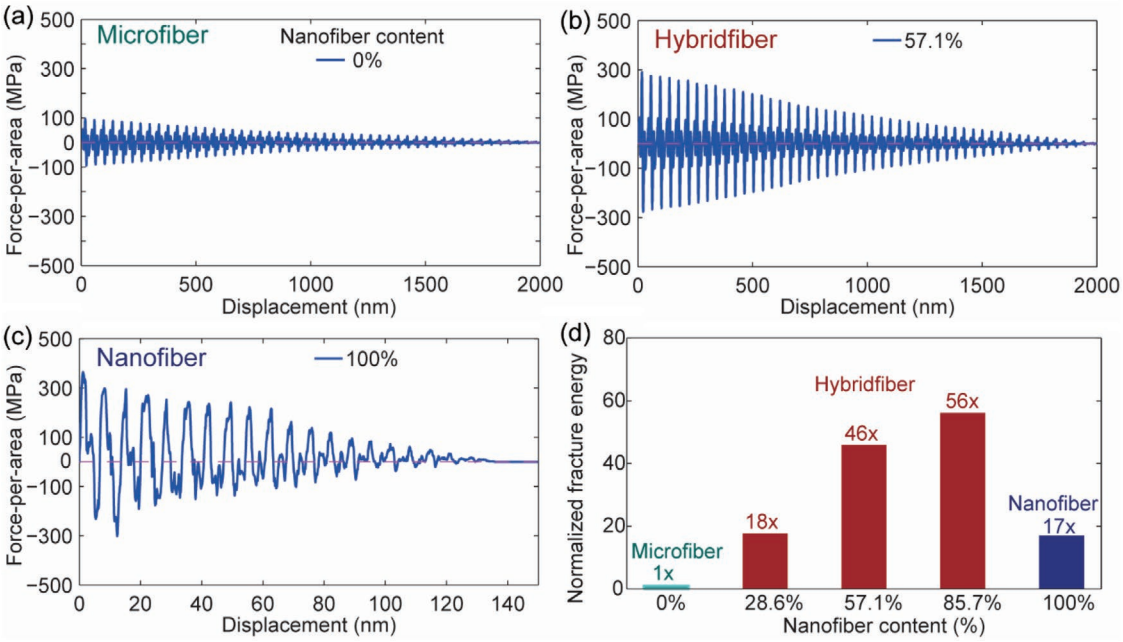

Figure 3. Force per area as the function of displacement for cellulose fibers with different nanofiber contents: a) 0% (100% microfiber), b) 57.1%, and c) 100%. d) Normalized fracture energy for cellulose fibers with different nanofiber contents, taking the value of microfiber as the baseline.

the strong water stability of the sealing hydrogen bonding (Figure S11, Supporting Information). The cellulose nanofiber straw shows a much slower wetting due to the dense packing of nanofibers (Figure 2b) and the existence of carboxyl groups, with imbibed water barely going above the water level in the container along the straw after 30 min (Figure 4d). However, delamination occurs along the outer edge of cellulose nanofiber film, leading to the partial disintegration of the straw (Figure 4e). This could be attributed to the dissociation effects of water on the hydrogen bonds among the short cellulose nanofibers (Figure 4f). By contrast, the cellulose hybrid straw shows satisfactory water stability and wetting stability. After being immersed in water for 4 h, imbibed water in the straw barely go above the water level in the container along the straw and the straw retains its structural integrity without appreciable delamination (Figure 4h). The low wettability of the cellulose hybrid straw results from the dense packing of cellulose hybrid fibers (Figure 2c) comparable to that of the nanofibers, while the stable structural integrity can be understood as following. Even though water can be absorbed into the cellulose hybrid straw and cause the dissociation of some hydrogen bonds between the cellulose fibers, the cellulose microfibers are long enough so that they stay as an integral fiber network through the remaining hydrogen bonds along the microfibers (as illustrated in Figure 4i). Similar effect is observed in the cellulose microfiber straw, which remains bonded along the edge even though the whole straw is soaked and becomes soft, due to the similar mechanism (as illustrated in Figure 4c). We further use a pipette to create a vacuum to mimic human drinking through straw. Water can be sucked up through our cellulose hybrid straws after 4 h (Figure S12, Supporting Information).

The degradability of the cellulose-based straws is tested by placing the straws in a natural environment (University of Maryland campus) (Figure 4j). For comparison, we place a cellulose hybrid straw, a cellulose nanofiber straw, and a commercial plastic straw together at the same location. Cellulose microfiber straws are not tested due to their poor mechanical performance and water stability. After ≈30 days, the cellulose nanofiber straw starts to delaminate, gradually fragments, and disappears after ≈2 months. The cellulose hybrid straw starts to delaminate after ≈70 days and then disintegrates into fragments after ≈4 months. The stability of straws (in moisture) is closely related with the hydrogen bonding stability in the atmospheric water. As illustrated in Figure 4f, water has the strongest dissociation effects on the hydrogen bonds among the short cellulose nanofibers. In natural environment, water can attack the hydrogen bonding in the short cellulose fibers much easier than that in the hybrid straw in which microfibers are long enough so that an integral fiber network can maintain longer. By contract, the commercial plastic straw, which usually takes hundreds of years to fully degrade, remained unchanged with no sign of degradation in 4 months during the test. The degradability of cellulose hybrid straws offers a unique advantage against the nondegradable plastic straw.

With the comprehensive studies of the properties and performance, compared with the plastic straws, the cellulose hybrid straws have several key properties to ensure their capability of replacing the plastic straws. 1) Cellulose hybrid straws show comparable mechanical strength to that of commercial plastic straws, ensuring their quality to replace the commercial straws. 2) Cellulose hybrid straws show high flexibility by mixing flexible long microfibers to the rigid nanofibers. After bending, no cracks were found on the hybrid straws, outperforming the commercial plastic straws. 3) Cellulose hybrid straws exhibit excellent hydrostability without delimitation for at least 4 h in

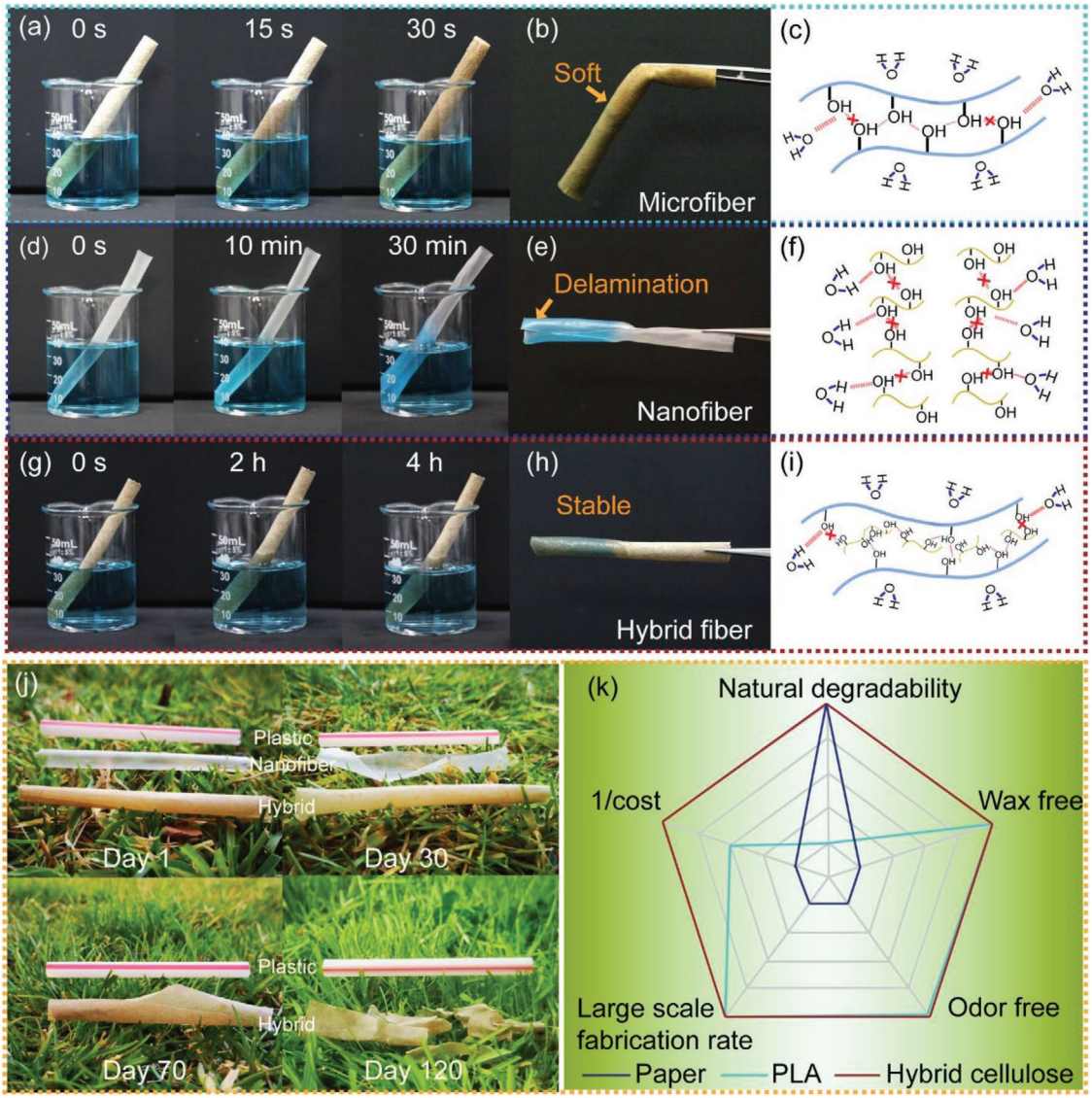

Figure 4. Water immersing test for a) microfiber straw, d) nanofiber straw, and g) cellulose hybrid straw. Straw status after immersing in water of b) microfiber straw for 30 s, e) nanofiber straw for 30 min, and h) cellulose hybrid straw for 4 h. Schematics of water attacking the hydrogen bonds for the hydrogen bonding networks of c) microfibers, f) nanofibers, and i) hybrid fibers. j) Degradation test for cellulose hybrid straw, nanofiber straw, and plastic straw. k) Radar plot to compare the cellulose hybrid straw with PLA straw and paper straw.

water and good wetting stability that water maintained at the drink level due to blocked capillary effect of densely packed cellulose nanofibers. 4) Cellulose hybrid straws are based on low-cost raw materials. Since bagasse is a waste byproduct from the sugarcane industry, the cost to produce microfibers is extremely low. In lab scale, each straw may only consume ≈200 mg cellulose nanofibers and ≈200 mg cellulose microfibers. Based on this, for each hybrid straw, the raw material costs as low as ≈0.06 cents (calculated according to ≈\$2.5 kg^{-1} for low-cost commercial nanofibers and ≈\$0.445 kg^{-1} for microfibers as reported based on energy and raw material cost[31]). Further reduction of cost is expected when scaling up in industry with better energy use in system and using low-cost raw materials, enabling the cost of cellulose straws competitive to or even lower than that of plastic straws (≈0.2 cents per plastic straw). More importantly, the relatively cheap cost of plastic straws today may bring serious environmental problems in the future that we will have to address at a prohibitive cost. With excellent stability and degradability and low-cost raw materials, cellulose hybrid straws are exceptional candidates to replace plastic straws.

Paper straws are the most widely used alternatives for plastic straws. To evaluate the performance of our as-prepared hybrid straws, we conduct the mechanical properties (dry and wet), hygroscopicity, and the water stability test and compare with commercial paper straw. For the mechanical properties, as shown in Figure S13 (Supporting Information), the tensile strength of hybrid cellulose film is 70 MPa, which is more than 2× higher than that of the commercial paper straw (≈32 MPa). In addition, the wet tensile strength of the two samples after immersing in water for half an hour is also measured and

the tensile strength of wet hybrid cellulose film is 14 MPa, which is 10× stronger than that of the commercial paper straw (≈1.4 MPa), as also shown in Figure S13 (Supporting Information). As shown in Figure S14 (Supporting Information), the wax layer of the commercial paper straw delaminates after immersing in water for 30 min and fluffy microfiber core is exposed, which is presumably the reason for the extremely low wet mechanical strength. The water stability comparison for the hybrid cellulose straw and the commercial paper straw immersed in water after 30 min is shown in Figure S15 (Supporting Information), and again the wax layer of the commercial paper straw delaminates and fluffy fibers are exposed and even dispersed in water, while our as-synthesized hybrid cellulose straw maintained good water stability during the 30 min test, presumably due to the more compacted cellulose fiber network and the existence of carboxyl groups. The hygroscopicity test is shown in Figure S16 (Supporting Information) that hybrid cellulose straw absorbs less water especially after the first 20 min when the wax layer starts to delaminate. The water absorption for both kinds of straws reaches equilibrium after ≈1 h and the hybrid cellulose straw absorbs 50% less water than the commercial paper straw (110% vs 160%). All the above results prove that compared with the commercial paper straws, the hybrid cellulose straws have better dry and wet mechanical strength and water stability, outperforming the commercial paper straws.

We further summarized a comprehensive comparison between the cellulose hybrid straw with two popular degradable straws (PLA straw and paper straw), on some other manufacturing and performance parameters such as their cost, natural degradability, wax cover, taste, and their possible large-scale production rate listed in Figure 4k. The cellulose hybrid straws again outperform PLA straws and the paper straws comprehensively in all the listed aspects. For instance, the cellulose hybrid straws (≈0.4 cents per straw) are potentially 5 times and 10 times lower in cost than PLA straw (≈2 cents per straw) and paper straw (≈4 cents per straw), respectively, solving a roadblock problem in cost for plastic replacement.[32] In addition, PLA straws cannot be degraded naturally but need a special facility to break them down that is not accessible in most countries. For the paper straws on the market, in order to solve the water stability problem, multilayers are assembled with water-resistance wax covering the outside of the paper tube core, not only raising the cost but also limiting the large-scale production rate. In addition, not only do paper straws show very bad durability in water since only microfiber was used, but the chemicals used from the pulp fabrication process bring unpleasant odor to the drink. The cellulose hybrid straws, on the contrary, solve almost all the main drawbacks suffered by PLA straws and paper straws, making them a better candidate to replace plastic straws. Finally, while companies have tried to use the sippy lid to solve the pollution problem from plastic straws, it brings other problems, as it is discommodious to the consumers with disability and ultimately more plastics are used.

3. Conclusion

In this work, we design a binder-free rolling up approach to fabricate all-natural cellulose-based straws composed of cellulose micro- and nano- hybrid fibers from bagasse as a promising candidate to replace petroleum-derived plastic straws. The cellulose hybrid straws show high mechanical durability and hydrostability due to the substantive, compact, and strong hydrogen bonding formed among cellulose hybrid structures. The cellulose hybrid straws possess 1) comparable or even better mechanical performances (high flexural strength of ≈7 MPa, high tensile strength of ≈70 MPa, and high bending flexibility without appreciable cracking or folding marks after bending) than plastic straws and 2) sufficient hydrostability without compromising the degradability. The supreme properties and low-cost raw materials make the cellulose hybrid straws a cost-effective replacement for the currently available degradable but expensive straws (e.g., PLA and paper straws). For the large-scale production, the existing paper straw machines could be readily adapted to produce cellulose hybrid straws, which could further drive down the manufacturing cost, a desirable feature toward widespread use of cellulose hybrid straws to replace plastic straws.

4. Experimental Section

Preparation of Cellulose Microfiber, Nanofiber, and Hybrid Straws: Bagasse was obtained from American Biocarbon. Microfibers were obtained by immersing the bagasse (15 g) in 10% NaOH solution (1 L) at 150 °C for 10 h to remove the greater part of lignin and hemicellulose. The mixture was then washed several times through filtration with distilled water and microfibers were dried in air and stored in the refrigerator. Nanofibers were obtained by TEMPO oxidation method from wood chips.[33–35] A total of 30 g of kraft bleached softwood pulp was suspended in 1500 mL deionized water containing 3 mmol TEMPO and 30 mmol NaBr. The TEMPO-mediated oxidation was initiated with the addition of 150 mmol NaClO. The pH was maintained at 10.0–10.5 with 1 mol L^{-1} NaOH solution. The whole process was maintained under stirring (IKA RW20 digital mixer) for 2–3 h. The resulting pulp was washed by filtration and stored in a cold room at 4 °C for further analysis and treatment. An aqueous solution of 1.0% concentrated fiber was then treated in a Microfluidizer processor M-110EH at 2k psi pressure.

To make straws, cellulose suspension containing 1.5 g cellulose in solid (microfiber, nanofiber, or mixed fiber, respectively) was blended well and vacuum filtrated into a wet film by using a funnel with 14 cm in diameter. Wet rectangular film strips (≈3 cm × 10 cm) were cut from the wet film and then rolled up on a PET stick. The edges of the film were sealed by simply pressing to adhere. After drying in the ambient atmosphere for several hours to form hydrogen bonds, the straw could be separated from the PET stick easily.

Mechanical Tests: The bending property of the straws and the tensile property of the cellulose films were measured by a Tinius Olsen H5KT tester. All the straw samples were placed in a conditioning chamber (25 °C and 50% relative humidity) until an equilibrium moisture content of 8% was achieved. The water content was measured by recording the mass of each sample before and after baking in oven set at 120 °C for 12 h to remove the free water molecules. The dimensions for tensile samples of microfiber films, nanofiber, and hybrid fiber were ≈20 mm by 5 mm by 0.23 mm, 20 mm by 5 mm by 0.09 mm, and 20 mm by 5 mm by 0.15 mm, respectively. It was noted that the same amount of cellulose fibers in the film fabrication process was used, so that the performance of different types of straws could be compared under the same material cost. The distinct micro-/nanoscale material structures of the three types of hybrids led to different thicknesses of the resulting cellulose films. Nanofibers were densely packed with a density of ≈0.94 g cm^{-3}, leading to the thinnest film, while microfibers were loosely packed with a density of only ≈0.31 g cm^{-3}, leading to the thickest film, and the hybrid fibers yielded a film with intermediate thickness.

Furthermore, all mechanical test results were normalized by the cross-session area of the straws, so that the comparison of the intrinsic mechanical properties became independent of the film thickness. The samples were clamped at both ends and stretched along the sample length direction until they fractured with a constant test speed of 2 mm min^{-1} at room temperature.

The length and inner diameter for all the straws were ≈10 cm and ≈8 mm. The outer diameters for cellulose microfiber straw, nanofiber straw, and hybrid straw were ≈8.5, 8.2, 8.3 mm, respectively. As shown in Figure S17 (Supporting Information), for the three-point bending test, the straw was placed and stabilized on two roller supports at a set distance of ≈30 mm. The beam rested above the two roller supports and was subjected to a concentrated load at the sample's center with a constant test speed of 2 mm min^{-1} at room temperature.

The flexure strength for hollow tube could be derived based on the following equation

$$\sigma_{\text{hollow}} = \frac{M \cdot y}{I} = \frac{\frac{F \cdot L}{4} \cdot y}{\frac{\pi \cdot \left[\left(\frac{D}{2}\right)^4 - \left(\frac{d}{2}\right)^4\right]}{4}} \quad (1)$$

where M is the maximum bending moment, I is the moment of inertia of cross-section, y is the maximum distance from the center of the tube (equals to d), l is the distance between the two points beneath the specimen, F is the applied force, D is the outer diameter of the straw, and d is the inner diameter of the straw.

Characterization: The morphologies of the cellulose fibers were measured by a SEM (Hitachi SU-70). AFM (Cypher ESTM Environmental) was applied to characterize the morphology of the nanofiber-coated mica wafer in tapping mode. The density of microfiber film, nanofiber film, cellulose hybrid film, and commercial plastic film was calculated based on the weight and dimensions of the film. The zeta potential was determined using a Zetasizer Nano ZS90 at pH = 7 and 0.5 wt% of nanofibers in distilled water.

MD Simulation: Considering the scale of simulation, large-scale MD simulations using the massively parallel simulator (LAMMPS)[36] were performed on CG scheme to understand the influence of nanofiber content to mechanical properties, which could take advantage of computational resource reasonably. There were 3 levels in the coarse-grained scheme to calculate the mechanical properties of cellulose fiber. All the CG parameters were derived from the explicit hydrogen bond energy term of the REAX potential[37] at the atomistic level. For this level-1 CG scheme, the atom assembly of anhydroglucose monomer ($C_6H_{10}O_5$) was coarse-grained and represented as a "bead," so that the whole chain could be coarse-grained into a chain of beads. Elastic network model force constants were obtained directly from the variance–covariance matrix calculated from fully atomic molecular dynamics.[38] For level 2 CG, a model was constructed that comprised of 36 level-1 beaded chains based on the crystalline cellulose structure. The cross-section of such a model was ≈1.6 nm by ≈6 nm, in close agreement with the experimental results.[39] The CG bead length for level 2 would be ≈3.384 nm. For level 3 CG, the beads of crystalline cellulose were constructed with 7 level-2 beaded chains, leading to a ribbon cross-section of ≈4 nm by ≈137 nm, as suggested by experimental observations.[39] The CG bead length for level 3 would be ≈20.304 nm. This CG method was widely used to present the key mechanical properties of cellulose fiber with a large scale.[40] The sizes of micro and nano CG beads could be obtained as 20.304 and 3.384 nm, respectively. Due to only part of hydroxyl groups forming the hydrogen bond in the straw, the potential energies on the CG scheme were set as E(nano) = 34.7697 kcal $mole^{-1}$ and E(nano) = 212.97 kcal $mole^{-1}$ to represent microfiber and nanofiber, respectively. Thus, the potential energy of hybrid fibers could be obtained as $E(\text{hybrid}) = \sqrt{E(\text{micro}) \times E(\text{nano})}$, through the customary Lorentz–Berthelot mixing rules.[30] All cellulose materials showed shear failure.[30] Replacing the different amounts of microfiber with several nanofibers could construct the hybrid straw modeling with different nanofiber contents (Figure S8, Supporting Information). Here, the nanofiber content was defined as

$$\psi = \frac{m_{\text{nanofiber}}}{m_{\text{total}}} \times 100\% \quad (2)$$

where $m_{\text{nanofiber}}$ and m_{total} represent the mass of nanofiber and the whole fibers in straw, respectively. A Nose–Hoover thermostat was used to maintain the *NVT* ensembles at 5 K in the process of relaxing and pulling, for the purpose of suppressing thermal noise to clearly reveal the fine feature of the hydrogen bond stick-slip event. The timestep was set as 0.25 fs and the nonperiodic boundary conditions were applied in all directions. All the calculations were relaxed using the conjugate gradient algorithm to minimize the total energy of the system until the total atomic forces were converged to less than 10^{-11} eV $Å^{-1}$. Displacement loading was applied to the end of the circumambient fibers with the velocity of 0.001 Å fs^{-1} and the first bead of middle fiber was fixed. Thus, the force (F) was calculated by summing up the force component along the sliding direction of all the beads in the middle fiber. The stress could be obtained by

$$\sigma_{\text{ave}} = F/A \quad (3)$$

where A represents the section area of the middle chain.

Supporting Information

Supporting Information is available from the Wiley Online Library or from the author.

Acknowledgements

This work had no direct funding support. The authors acknowledge the use and support of the Maryland NanoCenter and its AIMLab. The authors also acknowledge Ruiyu Mi on her help on the AFM measurement on cellulose nanofibers. The authors acknowledge the University of Maryland supercomputing resources (http://hpcc.umd.edu) made available for conducting the simulation research reported in this paper.

Conflict of Interest

The authors declare no conflict of interest.

Author Contributions

X.W. and Z.P. contributed equally to this work. L.H., T.L., and X.W. conceived the idea and designed the present work. X.W., Q.X., R.W., and C.L. carried out the cellulose fiber preparation and straw fabrication. X.W., C.C., W.G., and U.R. contributed to mechanical measurements. Z.P., U.R., and T.L. contributed to both the mechanical simulations and analysis. X.W., Y.Z., and C.C. performed detailed microscopic characterization. All authors discussed the results and contributed to the final paper.

Keywords

cellulose, coarse-grained modeling, sustainable materials

Received: December 15, 2019
Revised: February 18, 2020
Published online: April 6, 2020

[1] xxxx, *Nat. Commun.* **2018**, *9*, 2157.
[2] K. L. Law, S. Moret-Ferguson, N. A. Maximenko, G. Proskurowski, E. E. Peacock, J. Hafner, C. M. Reddy, *Science* **2010**, *329*, 1185.
[3] K. L. Law, S. E. Moret-Ferguson, D. S. Goodwin, E. R. Zettler, E. De Force, T. Kukulka, G. Proskurowski, *Environ. Sci. Technol.* **2014**, *48*, 4732.
[4] L. Gu, T. Ozbakkaloglu, *Waste Manage.* **2016**, *51*, 19.
[5] R. Geyer, J. R. Jambeck, K. L. Law, *Sci. Adv.* **2017**, *3*, e1700782.
[6] D. Hoornweg, P. Bhada-Tata, C. Kennedy, *Nature* **2013**, *502*, 615.
[7] M. C. Rillig, *Environ. Sci. Technol.* **2012**, *46*, 6453.
[8] C. M. Rochman, A. M. Cook, A. A. Koelmans, *Environ. Toxicol. Chem.* **2016**, *35*, 1617.
[9] M. A. Browne, T. S. Galloway, R. C. Thompson, *Environ. Sci. Technol.* **2010**, *44*, 3404.
[10] J. R. Jambeck, R. Geyer, C. Wilcox, T. R. Siegler, M. Perryman, A. Andrady, R. Narayan, K. L. Law, *Science* **2015**, *347*, 768.
[11] R. E. J. Schnurr, V. Alboiu, M. Chaudhary, R. A. Corbett, M. E. Quanz, K. Sankar, H. S. Srain, V. Thavarajah, D. Xanthos, T. R. Walker, *Mar. Pollut. Bull.* **2018**, *137*, 157.
[12] X. Zhang, W. Liu, D. Yang, X. Qiu, *Adv. Funct. Mater.* **2019**, *29*, 1806912.
[13] P. Song, H. Wang, *Adv. Mater.* **2019**, 1901244.
[14] A. Pandey, C. R. Soccol, P. Nigam, V. T. Soccol, *Bioresour. Technol.* **2000**, *74*, 69.
[15] K. H. Gardner, J. Blackwell, *Biochim. Biophys. Acta, Gen. Subj.* **1974**, *343*, 232.
[16] H. L. Zhu, W. Luo, P. N. Ciesielski, Z. Q. Fang, J. Y. Zhu, G. Henriksson, M. E. Himmel, L. B. Hu, *Chem. Rev.* **2016**, *116*, 12650.
[17] D. Klemm, B. Heublein, H. P. Fink, A. Bohn, *Angew. Chem., Int. Ed.* **2005**, *44*, 3358.
[18] M. A. S. A. Samir, F. Alloin, A. Dufresne, *Biomacromolecules* **2005**, *6*, 612.
[19] C. Jia, C. J. Chen, Y. D. Kuang, K. Fu, Y. L. Wang, Y. G. Yao, S. Kronthal, E. Hitz, J. W. Song, F. J. Xu, B. Y. Liu, L. B. Hu, *Adv. Mater.* **2018**, *30*, 1801347.
[20] A. Pandey, C. R. Soccol, P. Nigam, V. T. Soccol, L. P. S. Vandenberge, R. Mohan, *Bioresour. Technol.* **2000**, *74*, 81.
[21] J. W. Song, C. J. Chen, C. W. Wang, Y. D. Kuang, Y. F. Li, F. Jiang, Y. J. Li, E. Hitz, Y. Zhang, B. Y. Liu, A. Gong, H. Y. Bian, J. Y. Zhu, J. H. Zhang, J. Li, L. B. Hu, *ACS Appl. Mater. Interfaces* **2017**, *9*, 23520.
[22] R. M. Rowell, *Handbook of Wood Chemistry and Wood Composites*, 2nd ed., CRC Press, Boca Raton, FL **2012**.
[23] F. Jiang, T. Li, Y. J. Li, Y. Zhang, A. Gong, J. Q. Dai, E. Hitz, W. Luo, L. B. Hu, *Adv. Mater.* **2018**, *30*, 1.
[24] Z. Q. Fang, H. L. Zhu, W. Z. Bao, C. Preston, Z. Liu, J. Q. Dai, Y. Y. Li, L. B. Hu, *Energy Environ. Sci.* **2014**, *7*, 3313.
[25] Z. Q. Fang, H. L. Zhu, C. Preston, X. G. Han, Y. Y. Li, S. W. Lee, X. S. Chai, G. Chen, L. B. Hu, *J. Mater. Chem.* **2013**, *1*, 6191.
[26] S. Kalia, S. Boufi, A. Celli, S. Kango, *Colloid Polym. Sci.* **2014**, *292*, 5.
[27] D. H. Page, F. Elhosseiny, *Pulp Pap. Can.* **1983**, *84*, Tr99.
[28] C. C. Sun, *Int. J. Pharm.* **2008**, *346*, 93.
[29] L. Q. Jin, Y. W. Wei, Q. H. Xu, W. R. Yao, Z. L. Cheng, *J. Appl. Polym. Sci.* **2014**, *131*, 40450.
[30] H. L. Zhu, S. Z. Zhu, Z. Jia, S. Parvinian, Y. Y. Li, O. Vaaland, L. B. Hu, T. Li, *Proc. Natl. Acad. Sci. USA* **2015**, *112*, 8971.
[31] C. A. de Assis, M. C. Iglesias, M. Bilodeau, D. Johnson, R. Phillips, M. S. Peresin, E. M. Bilek, O. J. Rojas, R. Venditti, R. Gonzalez, *Biofuels, Bioprod. Biorefin.* **2018**, *12*, 251.
[32] E. Products, Prices for compostable straws, http://www.ecoproductsstore.com/compostable_straws.html (accessed: October 2019).
[33] A. Isogai, T. Saito, H. Fukuzumi, *Nanoscale* **2011**, *3*, 71.
[34] T. Paakkonen, K. Dimic-Misic, H. Orelma, R. Ponni, T. Vuorinen, T. Maloney, *Cellulose* **2016**, *23*, 277.
[35] Y. B. Zhou, C. J. Chen, S. Z. Zhu, C. Sui, C. Wang, Y. D. Kuang, U. Ray, D. P. Liu, A. Brozena, U. H. Leiste, N. Quispe, H. Guo, A. Vellore, H. A. Bruck, A. Martini, B. Foster, J. Lou, T. Li, L. B. Hu, *Mater. Today* **2019**, *30*, 17.
[36] S. Plimpton, *J. Comput. Phys.* **1995**, *117*, 1.
[37] T. R. Mattsson, J. M. D. Lane, K. R. Cochrane, M. P. Desjarlais, A. P. Thompson, F. Pierce, G. S. Grest, *Phys. Rev. B* **2010**, *81*, 5.
[38] D. C. Glass, K. Moritsugu, X. L. Cheng, J. C. Smith, *Biomacromolecules* **2012**, *13*, 2634.
[39] R. M. Brown, J. H. M. Willison, C. L. Richardson, P. Natl, *Proc. Natl. Acad. Sci. USA* **1976**, *73*, 4565.
[40] B. X. Fan, J. K. Maranas, *Cellulose* **2015**, *22*, 31.

ADVANCED FUNCTIONAL MATERIALS

Supporting Information

for *Adv. Funct. Mater.*, DOI: 10.1002/adfm.201910417

All-Natural, Degradable, Rolled-Up Straws Based on Cellulose Micro- and Nano-Hybrid Fibers

Xizheng Wang, Zhenqian Pang, Chaoji Chen, Qinqin Xia, Yubing Zhou, Shuangshuang Jing, Ruiliu Wang, Upamanyu Ray, Wentao Gan, Claire Li, Gegu Chen, Bob Foster, Teng Li, and Liangbing Hu**

Supplemental Materials

All Natural, Degradable, Rolled-Up Straws Based on Hybrid Micro-Nano Cellulose

Xizheng Wang,[1,2,a] Zhenqian Pang,[2,a] Chaoji Chen,[1] Qinqin Xia,[1] Yubing Zhou,[1,2] Shuangshuang Jing,[1] Ruiliu Wang,[1] Upamany Ray,[2] Wentao Gan,[1] Claire Li,[1] Gegu Chen,[1] Bob Foster,[3] Teng Li,[2,*] Liangbing Hu[1,*]

1. Department of Materials Science and Engineering, University of Maryland, College Park, Maryland, 20742
2. Department of Mechanical Engineering, University of Maryland, College Park, Maryland, 20742
3. Trinity Industries, Inc., Dallas, TX 75207, United States

[*] Corresponding authors. Email: Hu, L. (binghu@umd.edu), Li, T. (lit@umd.edu)

[a] These authors contributed equally to this work.

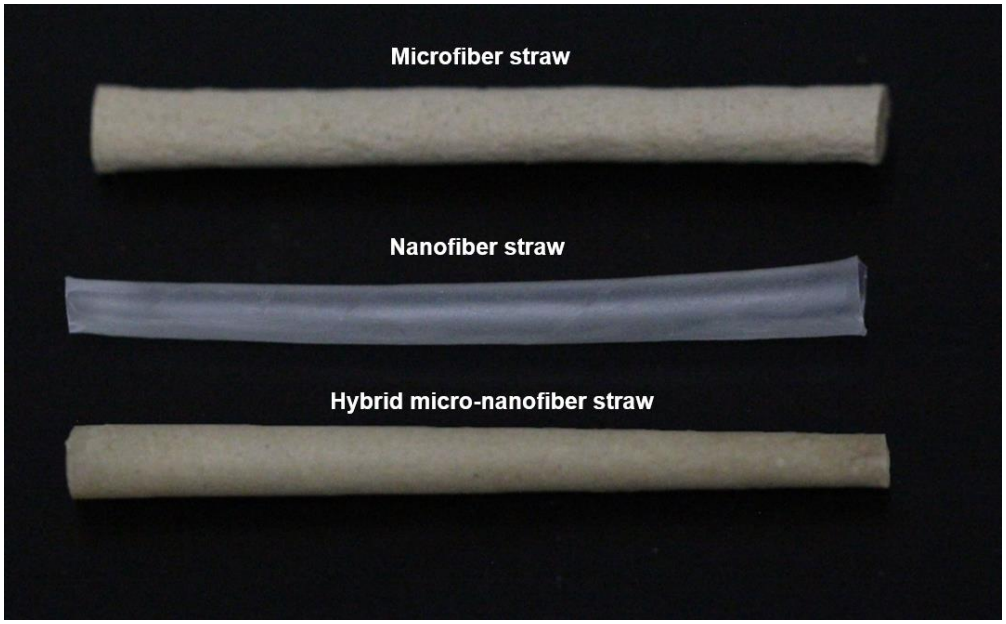

Figure S1. Direct comparison of cellulose microfiber straw, hybrid straw and nanofiber straw. Pure microfiber straws are opaque and as soft as regular paper. Pure nanofiber straws show some optical transparence due to the densely packed nanofibers and small interstices size. The produced hybrid micro-nano straws are opaque and has better mechanical strength than microfiber straws.

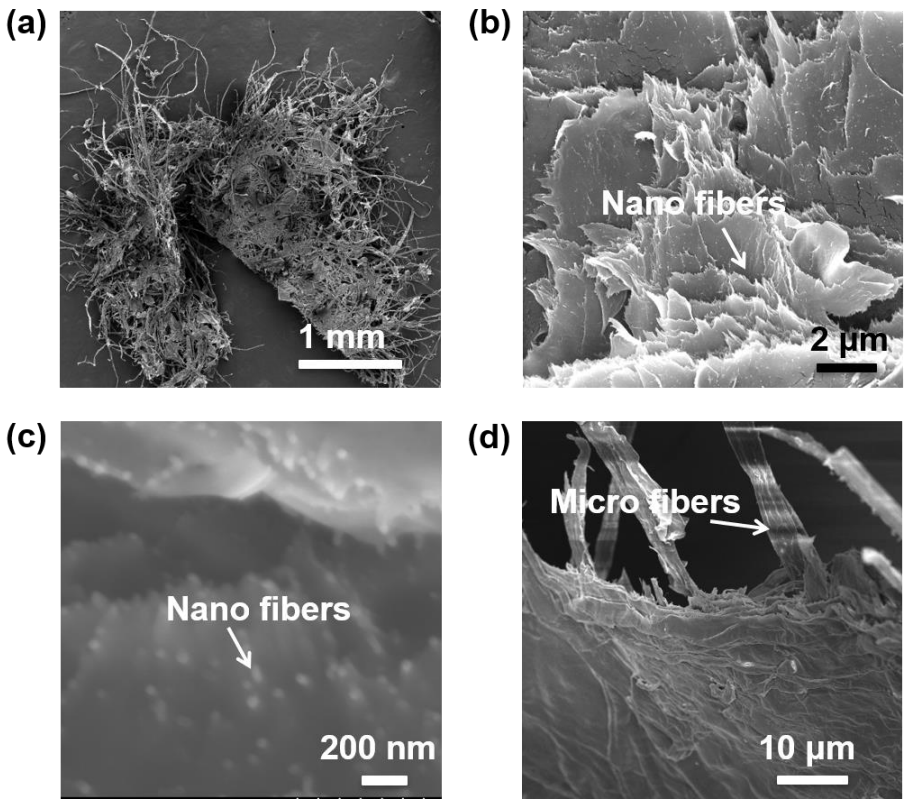

Figure S2. SEM of a. microfibers and the length can be several millimeters. b. the detail structure of nanofibers in the fracture surface of nanofiber film. c. Zoomed in morphology of nanofibers. d. the fracture edge surface of hybrid micro-nano fibers show that microfibers and nanofibers are fully mixed.

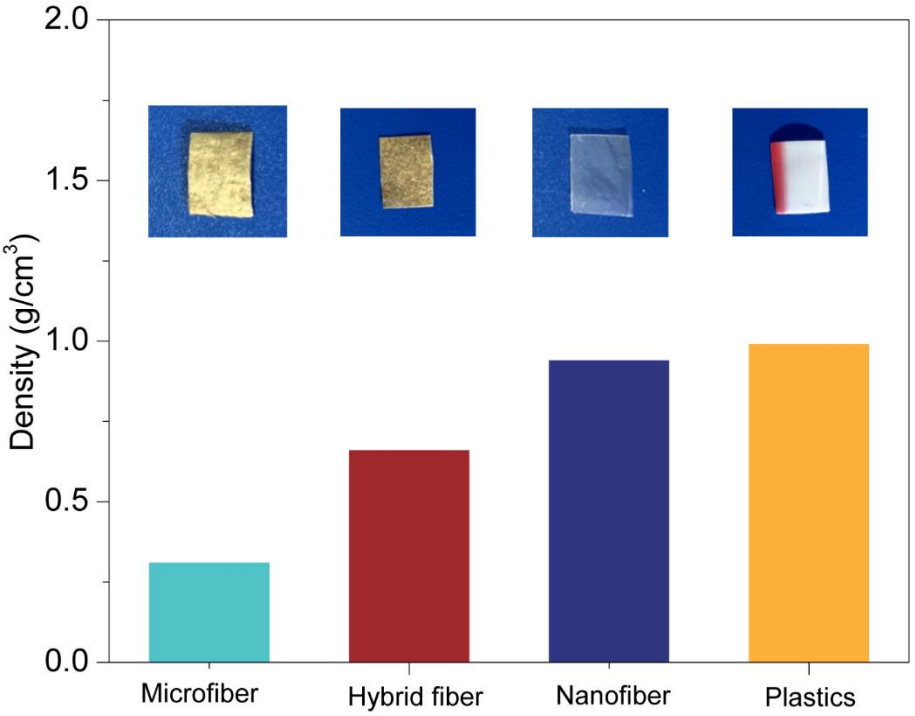

Figure S3. Density comparison of microfiber film, nanofiber film, cellulose hybrid film and commercial plastic film.

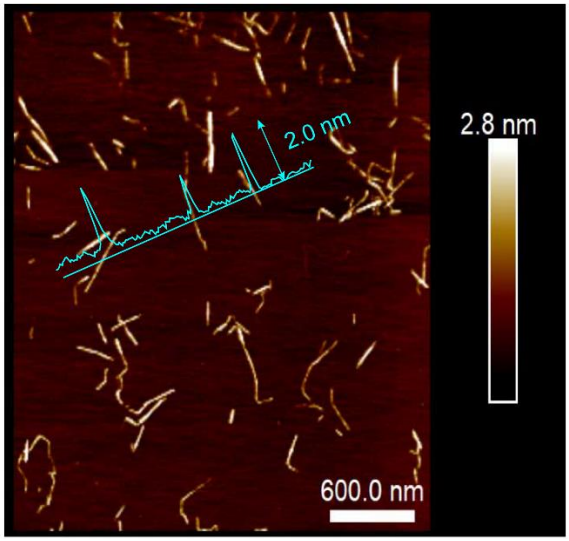

Figure S4. AFM image of cellulose nanofibers with a mean diameters of ~2 nm and a mean length of 100-700 nm.

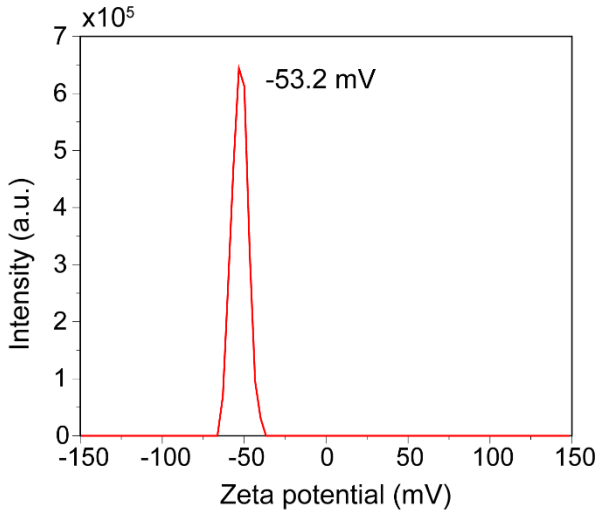

Figure S5. Zeta potential of the nanofiber (PH=7, 0.5 wt.%), indicating the existence of carboxyl groups.

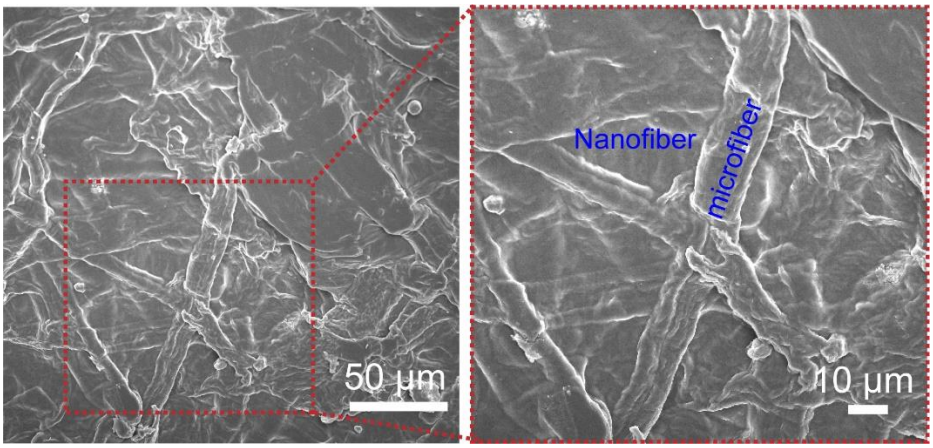

Figure S6. SEM images of hybrid cellulose fibers in different magnifications (1k and 2k). The microfibers and nanofibers are homogeneously mixed and the nanofibers fill the voids between microfibers, making the hybrid film dense.

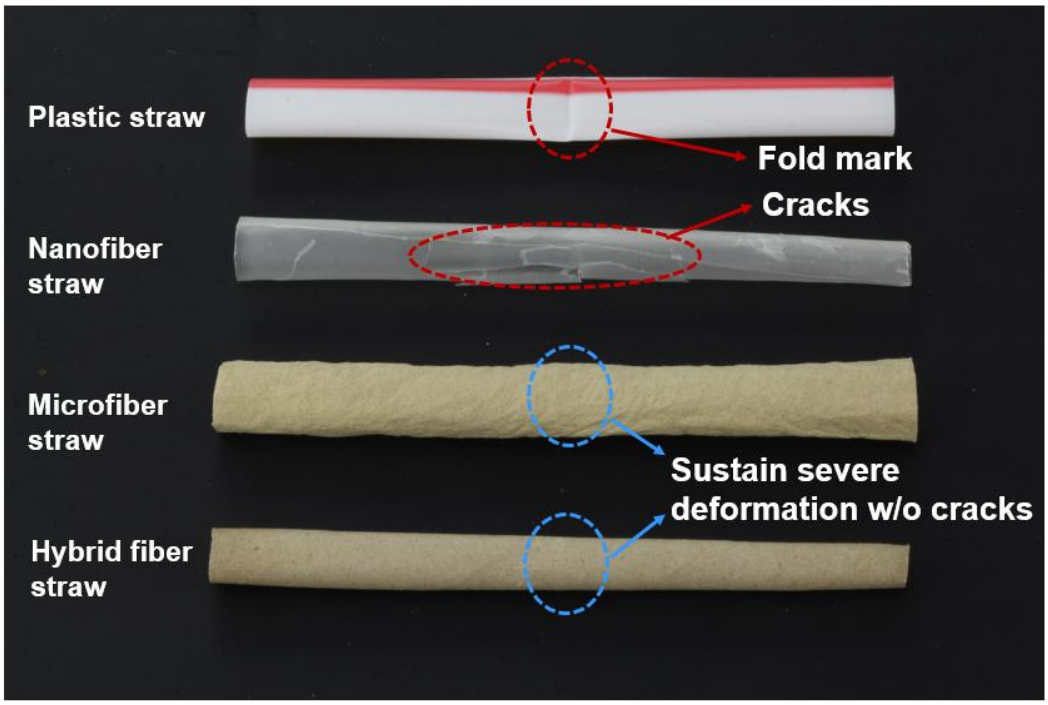

Figure S7. Different straws after bending. Nanofibers straw cracked severely, and plastic straw has bending marks. However cellulose microfiber straw and hybrid straw have no bending cracks after severe deformation, indicating their high flexibility.

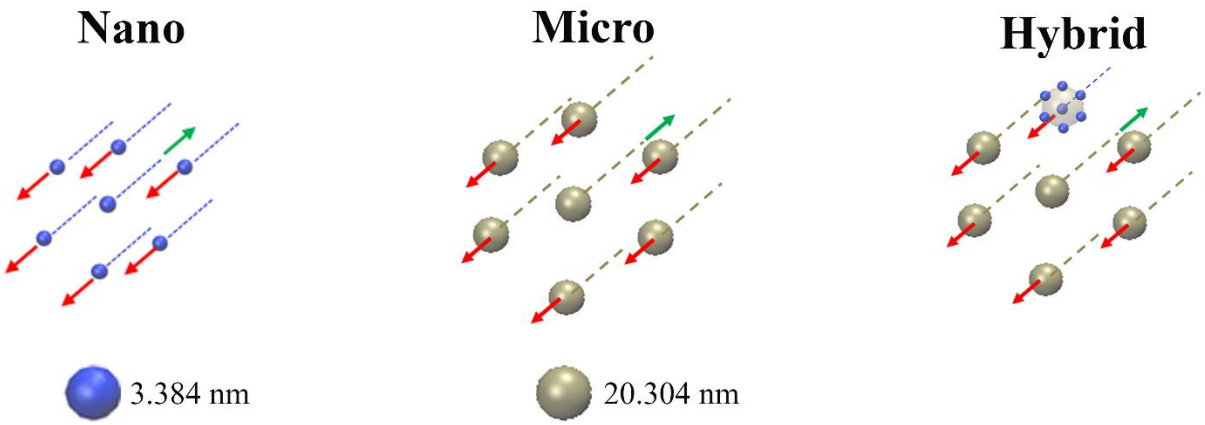

Figure S8. Schematics of the simulation models for cellulose nanofibers, microfibers and hybrid fibers. Colored circles represent the CG beads with different sizes.

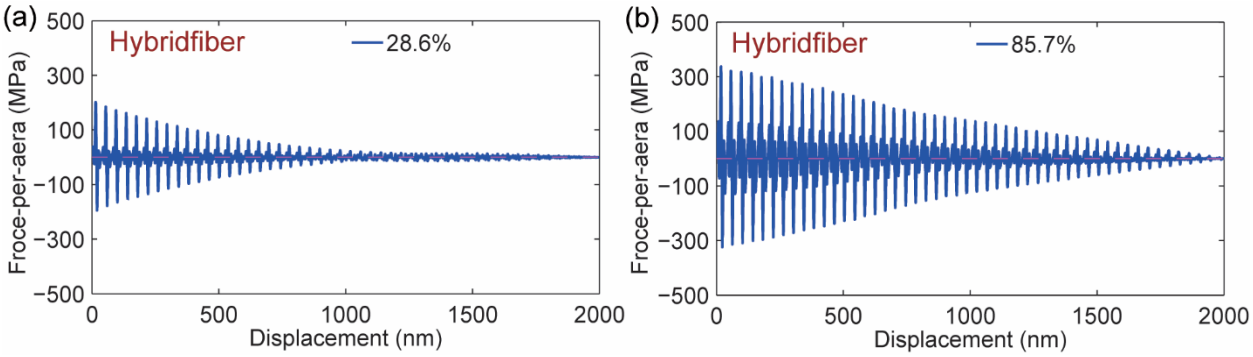

Figure S9. Force-per-area as the function of displacement for cellulose fibers with different nanofiber content (a) 28.6% and (b) 85.7%.

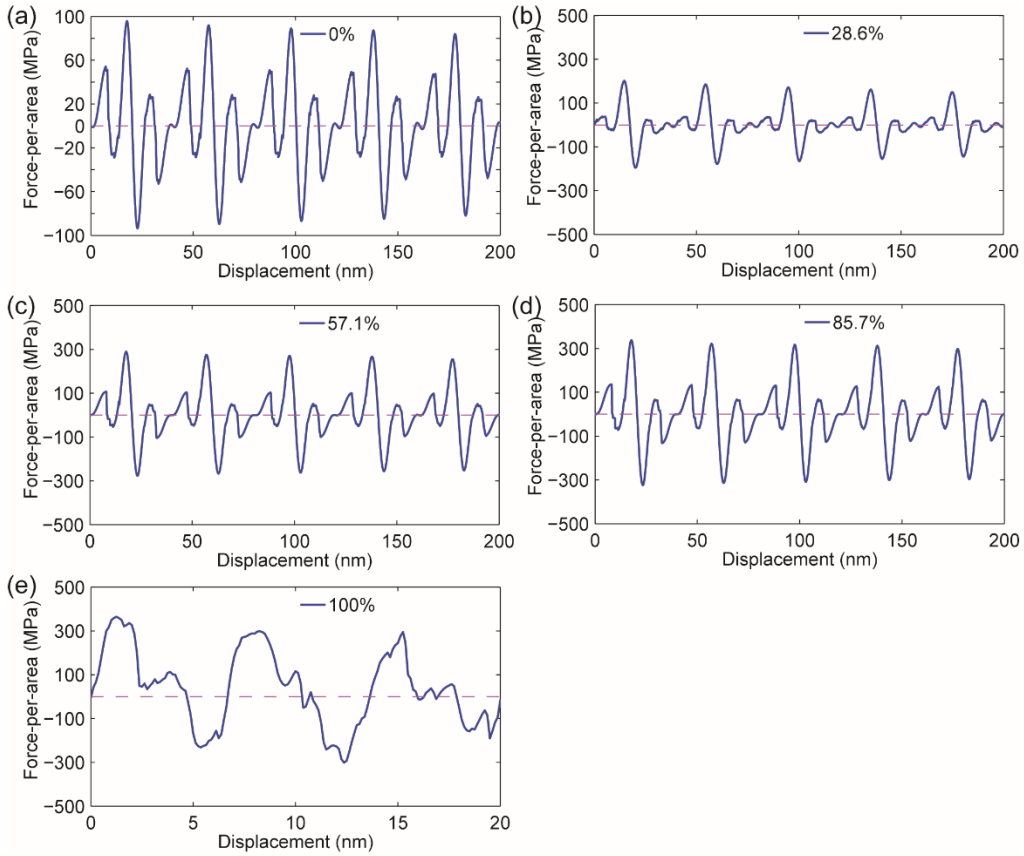

Figure S10. (a)~(e) Segment of force-per-area vs. displacement curves for different nanofiber content. The integration of the positive part of the curve is the fracture energy.

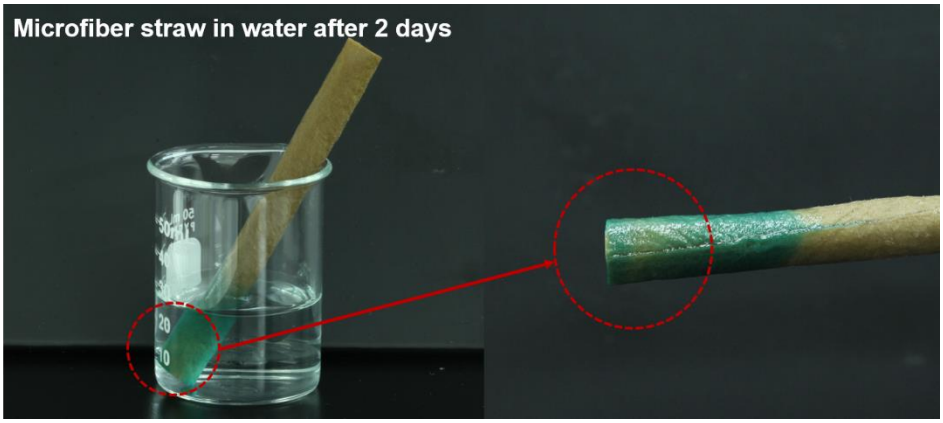

Figure S11. Microfiber straws in water after 2 day, still maintaining the tube shape.

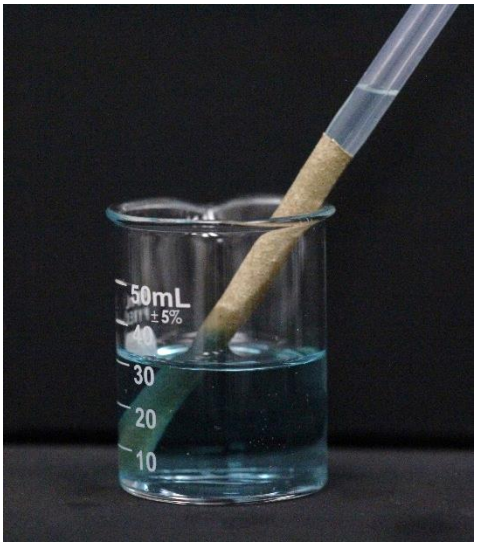

Figure S12. Hybrid micro-nano straws in water after 4 hours, and water can be soaked up, indicating the hybrid micro-nano straws have good water stability and wetting stability.

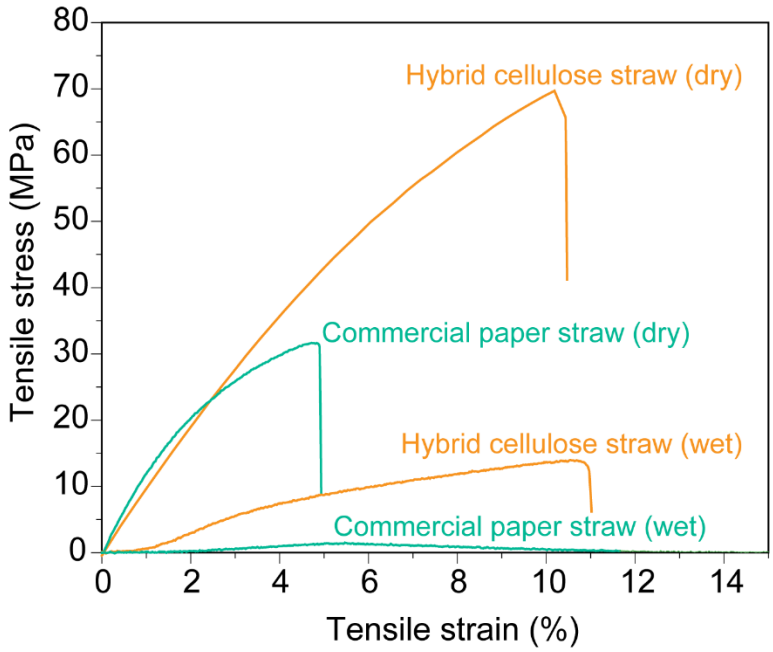

Figure S13. Tensile stress-strain curves of dry and wet hybrid cellulose straw film and commercial paper straw film. Hybrid cellulose straw shows both higher dry (2X) and wet (10X) tensile strengths than those of the commercial paper straw.

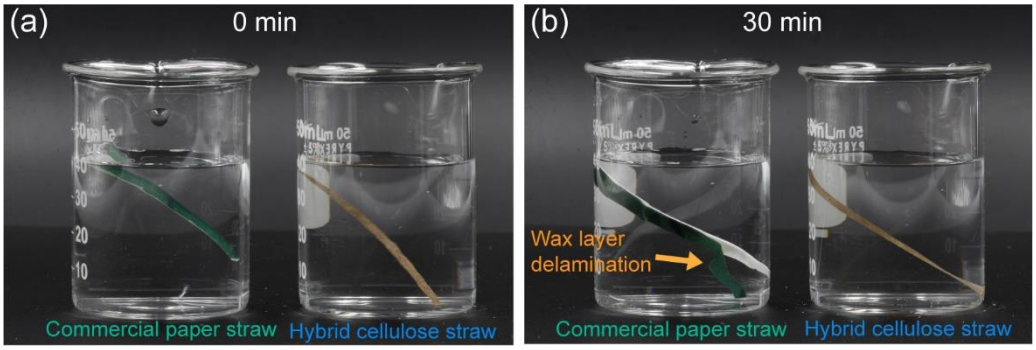

Figure S14. Commercial paper straw film and hybrid cellulose straw film immersed in water at (a) 0 min and (b) after 30 min. For commercial paper straw, the wax layer delaminates and fluffy cellulose fibers are exposed. By contrast, our hybrid cellulose straw film maintains good water stability during the 30 min immersion test.

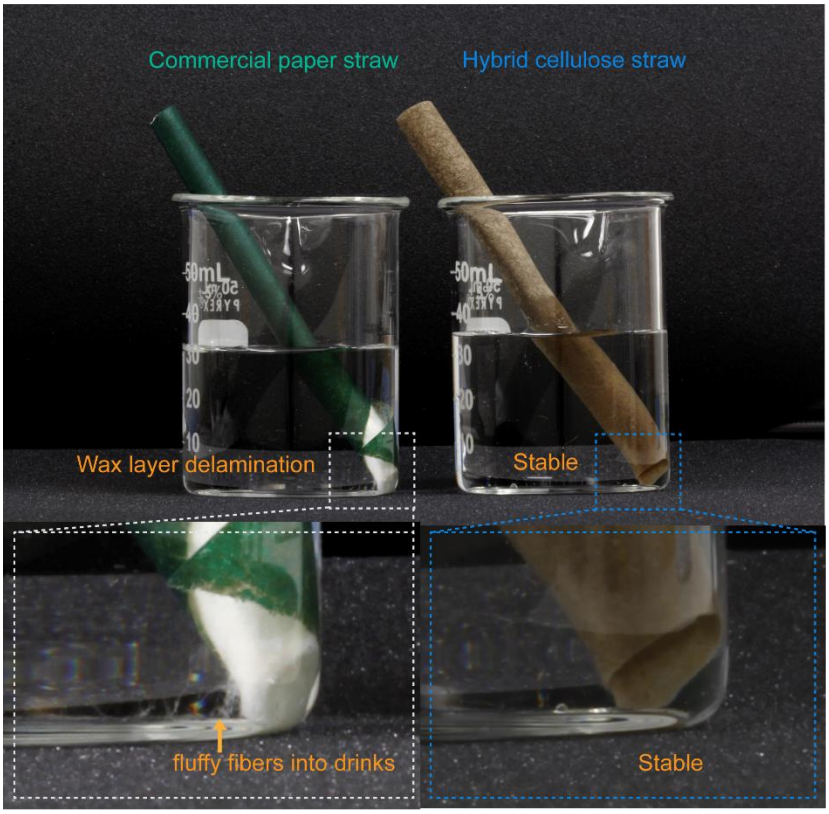

Figure S15. Water immersion test for commercial paper straw and hybrid cellulose straw. The wax layer of the commercial paper straw delaminates so that fluffy fibers are exposed and even dispersed in water. By contrast, our as-synthesized hybrid cellulose straw maintains good water stability during the 30 min immersion test.

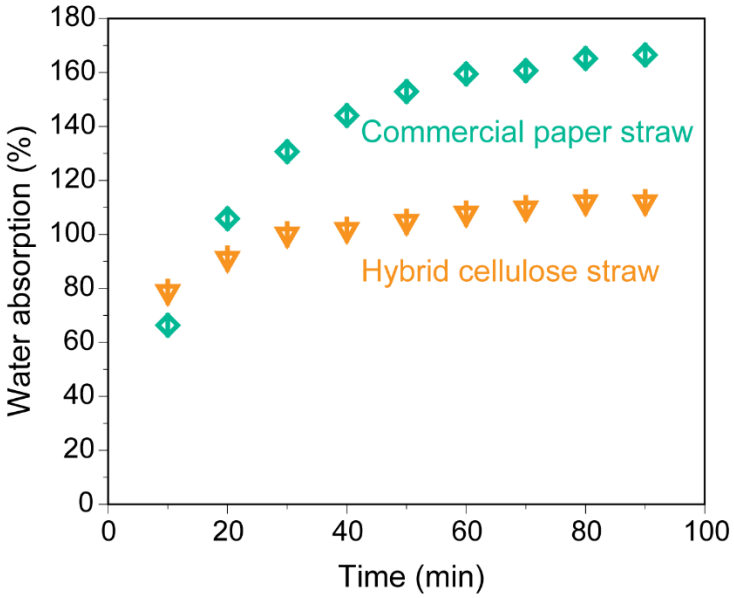

Figure S16. Water adsorption curves of commercial paper straw and hybrid cellulose straw over time. The water absorption of hybrid cellulose straw is lower than the commercial paper straw, justifying the better water stability of the hybrid cellulose straw.

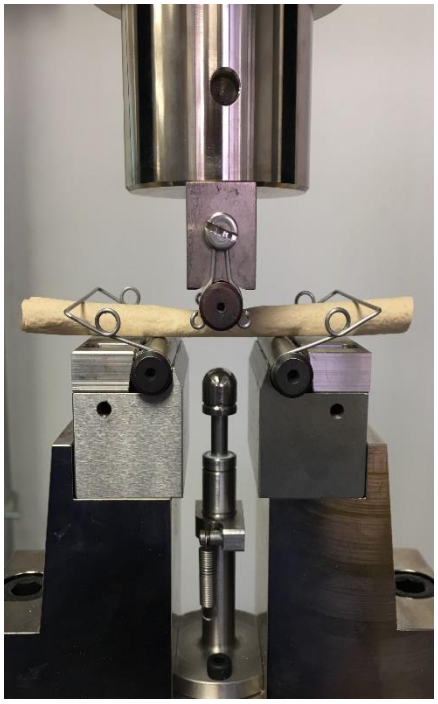

Figure S17. Photograph of three points bending test, which is used to measure the flexure streng